The Astrophysical Journal Letters, 714:L118–L122, 2010 May 1 doi:10.1088/2041-8205/714/1/L118

DIFFERENT STAR FORMATION LAWS FOR DISKS VERSUS STARBURSTS AT LOW AND HIGH REDSHIFTS

E. Daddi[1], D. Elbaz[1], F. Walter[2], F. Bournaud[1], F. Salmi[1], C. Carilli[3], H. Dannerbauer[1], M. Dickinson[4], P. Monaco[5], and D. Riechers[6,7]
[1] Laboratoire AIM, CEA/DSM-CNRS-Université Paris Diderot, Irfu/Service d'Astrophysique, CEA Saclay, Orme des Merisiers, 91191 Gif-sur-Yvette Cedex, France; edaddi@cea.fr
[2] Max-Planck-Institut für Astronomie, Königstuhl 17, D-69117 Heidelberg, Germany
[3] National Radio Astronomy Observatory, P.O. Box 0, Socorro, NM 87801, USA
[4] NOAO, 950 North Cherry Avenue, Tucson, AZ 85719, USA
[5] INAF-Osservatorio Astronomico di Trieste, Trieste, Italy
[6] Caltech, Pasadena, CA 91125, USA
Received 2009 December 17; accepted 2010 March 22; published 2010 April 5

ABSTRACT

We present evidence that bona fide disks and starburst systems occupy distinct regions in the gas mass versus star formation rate (SFR) plane, both for the integrated quantities and for the respective surface densities. This result is based on carbon monoxide (CO) observations of galaxy populations at low and high redshifts, and on the current consensus for the CO luminosity to gas mass conversion factors. The data suggest the existence of two different SF regimes: a long-lasting mode for disks and a more rapid mode for starbursts, the latter probably occurring during major mergers or in dense nuclear SF regions. Both modes are observable over a large range of SFRs. The detection of CO emission from distant near-IR selected galaxies reveals such bimodal behavior for the first time, as they allow us to probe gas in disk galaxies with much higher SFRs than are seen locally. The different regimes can potentially be interpreted as the effect of a top-heavy initial mass function in starbursts. However, we favor a different physical origin related to the fraction of molecular gas in dense clouds. The IR luminosity to gas mass ratio (i.e., the SF efficiency) appears to be inversely proportional to the dynamical (rotation) timescale. Only when accounting for the dynamical timescale, a universal SF law is obtained, suggesting a direct link between global galaxy properties and the local SFR.

Key words: cosmology: observations – galaxies: evolution – galaxies: formation – galaxies: starburst – infrared: galaxies

Online-only material: color figures

1. INTRODUCTION

Exploring the relation between the gas content and star formation rate (SFR) of galaxies is crucial to understanding galaxy formation and evolution. This is required to understand the nature of SF, the parameters that regulate it, and its possible dependence on local and global galaxy properties (e.g., Silk 1997; Elmegreen 2002; Krumholz & Thompson 2007; McKee & Ostriker 2007). In addition, this information is a critical ingredient of theoretical models of galaxy formation, either based on semianalytical realizations or on numerical simulations (e.g., Guiderdoni et al. 1998; Somerville et al. 2001; Monaco et al. 2007; Ocvirk et al. 2008; Dekel et al. 2009; Gnedin et al. 2009; Croton et al. 2006). In fact, the physics associated with the conversion of gas into stars inside galaxies is overwhelmingly complicated, so that theoretical models generally resort to scaling laws that are calibrated using observations of nearby galaxies.

Schmidt (1959) first suggested the existence of a power-law relation between surface densities of SFR and gas masses. Kennicutt (1998, hereafter K98) presented a calibration of the Schmidt law with a slope of 1.4 in log space, which has since been the most widely used in the community. K98 fits the local populations of spiral galaxies and IR-luminous galaxies (LIRGs/ULIRGs), with the gas mass including both neutral (H I) and molecular (H_2) hydrogen for spirals, and molecular gas only for (U)LIRGs (as their H I content is likely negligible). The molecular gas component is routinely estimated using its most luminous tracer, carbon monoxide (CO), that is generally optically thick. This requires an empirical derivation of the conversion factor to derive molecular gas masses from CO luminosities ($\alpha_{\rm CO} = M_{\rm gas}/L'_{\rm CO}$). K98 used the Galactic value for all objects in his sample.

Downes & Solomon (1998) showed that $\alpha_{\rm CO}$ is smaller for local (U)LIRGs than for spirals, by about a factor of 6—see a detailed discussion and additional references in the review by Solomon & Vanden Bout (2005). Bouché et al. (2007) applied such different conversion factors for spirals and (U)LIRGs, resulting in a steeper relation with a slope of about 1.7. Observations of high-redshift submillimeter selected galaxies (SMGs) can also be fit by the same relation, following Tacconi et al. (2008) who argued that a ULIRG-like $\alpha_{\rm CO}$ is appropriate for SMGs. Integrated quantities, $L'_{\rm CO}$ and IR luminosities ($L_{\rm IR}$), also appear to follow a correlation with a slope of 1.7 (e.g., Solomon & Vanden Bout 2005; Greve et al. 2005). In the following discussion, we use a Chabrier (2003) initial mass function (IMF) and a standard *Wilkinson Microwave Anisotropy Probe* cosmology.

2. RELATIONS BETWEEN IR LUMINOSITY AND GAS MASSES

In this Letter, we explore the validity of the SF law further by including new observations of CO emission in distant near-IR selected galaxies at $z = 0.5$ and $z = 1.5$ (Daddi et al. 2008, 2010—hereafter D10; F. Salmi et al. 2010, in preparation).

[7] Hubble Fellow.

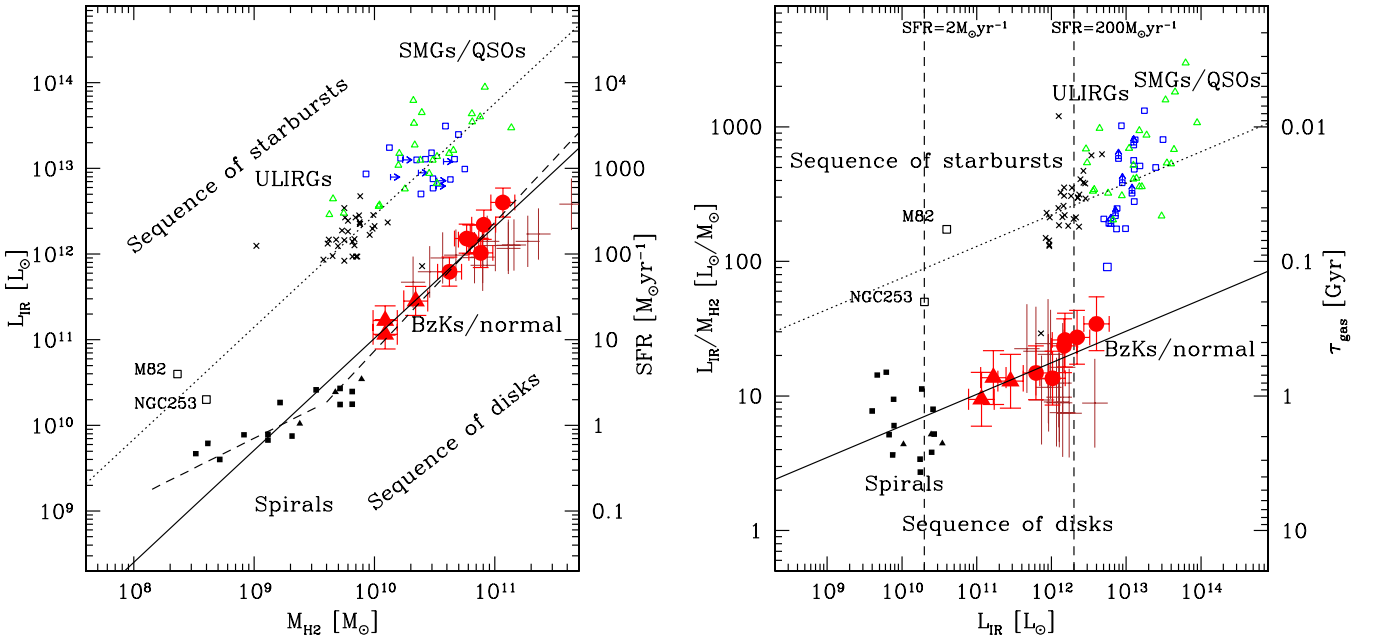

Figure 1. Comparison of molecular gas masses and total IR bolometric luminosities: BzK galaxies (red filled circles; D10), $z \sim 0.5$ disk galaxies (red filled triangles; F. Salmi et al. 2010, in preparation), $z = 1$–2.3 normal galaxies (Tacconi et al. 2010; brown crosses), SMGs (blue empty squares; Greve et al. 2005; Frayer et al. 2008; Daddi et al. 2009a, 2009b), QSOs (green triangles; see Riechers et al. 2006), local ULIRGs (black crosses; Solomon et al. 1997), and local spirals (black filled squares, Leroy et al. 2009; black filled triangles, Wilson et al. 2009). The two nearby starbursts M82 and the nucleus of NGC 253 are also shown (data from Weiß et al. 2001; Houghton et al. 1997; Kaneda et al. 2009). The solid line (Equation (1), slope of 1.31 in the left panel) is a fit to local spirals and BzK galaxies and the dotted line is the same relation shifted in normalization by 1.1 dex. The dashed line in the left panel is a possible double power-law fit to spirals and BzK galaxies. For guidance, two vertical lines indicate SFR = 2 and 200 $M_\odot$ yr^{-1} in the right panel.

(A color version of this figure is available in the online journal.)

These allow us to study more typical high-redshift galaxies with SFRs much larger than those of local spirals but less extreme than those of distant SMGs. The sample of six CO-detected $z = 1.5$ normal (BzK-selected) galaxies is presented in D10. We also use CO detections of three near-IR selected disk galaxies at $z = 0.5$. A detailed discussion of the $z = 0.5$ data set will be presented elsewhere (F. Salmi et al. 2010, in preparation). For comparison, we also show measurements for normal CO-detected galaxies at $z = 1$–2.3 from Tacconi et al. (2010), although we do not use these in our analysis. These new observations are placed in context with the literature data for ULIRGs, SMGs, and local samples of disk galaxies.

In order to investigate the location of these populations of normal high-z galaxies in the gas mass versus SFR plane, either for the integrated properties or for the surface densities, a crucial ingredient is, again, the α_{CO} conversion factor. Comparing the dynamical and stellar mass estimates, D10 derive a high $\alpha_{CO} = 3.6 \pm 0.8\, M_\odot$ (K km s^{-1} pc^2)$^{-1}$ for the BzK galaxies[8], quite similar to that for local spirals ($\alpha_{CO} = 4.6$). This is not unexpected, given the evidence that the $z \sim 1.5$ near-IR selected galaxies appear to be high-redshift analogs of local disks with enhanced gas content (see, e.g., discussions in Daddi et al. 2008, 2010; Dannerbauer et al. 2009; Tacconi et al. 2010, and later in this Letter). In the following, we adopt this value of $\alpha_{CO} = 3.6$ for the $z = 0.5$–2.5 normal galaxies[9] and the "consensus" value for the other populations ($\alpha_{CO} = 4.6$ for local spirals, $\alpha_{CO} = 0.8$ for local (U)LIRGs and distant SMGs/QSOs), and explore the consequences for the relation between gas masses and IR luminosities/SFRs.

Figure 1 is equivalent to Figure 13 in D10, after replacing L'_{CO} with M_{H2}. The right panel shows the ratio of L_{IR} to M_{H2} plotted versus L_{IR}. The implied gas consumption timescales ($\tau_{gas} = M_{H2}/SFR$; right panel of Figure 1) are 0.3–0.8 Gyr for the BzK galaxies,[10] about 2–3 times that for spirals, and over 1 order of magnitude smaller for local (U)LIRGs and distant SMGs. In a simple picture, this finding can be interpreted in terms of two major SF modes: a long-lasting mode appropriate for disks, that holds for both local spirals and distant BzK galaxies, and a rapid *starburst* mode appropriate for ULIRGs, local starbursts like M82 or the nucleus of NGC 253, and distant SMGs/QSOs. For the disk galaxies we formally fit

$$\log L_{IR}/L_\odot = 1.31 \times \log M_{H2}/M_\odot - 2.09, \qquad (1)$$

with an error on the slope of 0.09 and a scatter of 0.22 dex. Combining ULIRGs and SMGs we find that they define a trend with a similar slope, but with about 10 times higher L_{IR} at fixed M_{H2}.

A similar picture applies to the surface densities (Figure 2). We here use the original K98 measurements for local spirals and (U)LIRGs, but apply our choice of α_{CO} and a Chabrier (2003) IMF. For consistency with the K98 relation, we measure Σ_{gas} adding H I and H_2 for spirals, and H_2 for IR-luminous galaxies, in Figures 2 and 3. The results would not change if we had used H_2 only for all galaxies. Values for SMGs are taken from Bouché et al. (2007). For the BzK galaxies, we derive gas and SFR surface densities using the UV rest-frame (SFR) sizes. These are consistent with the CO sizes (D10) but are

[8] This conversion factor refers to the total gas mass, including H I, H_2, and helium, in their proportion within the half-light radius.

[9] Tacconi et al. (2010) assume a similar factor.

[10] We apply a conversion SFR[$M_\odot$ yr^{-1}] = $10^{-10} \times L_{IR}/L_\odot$, treating the two quantities as equivalent. In the case that a significant active galactic nucleus (AGN) contribution affects L_{IR} (e.g., for the QSOs), SFRs would be correspondingly lower.

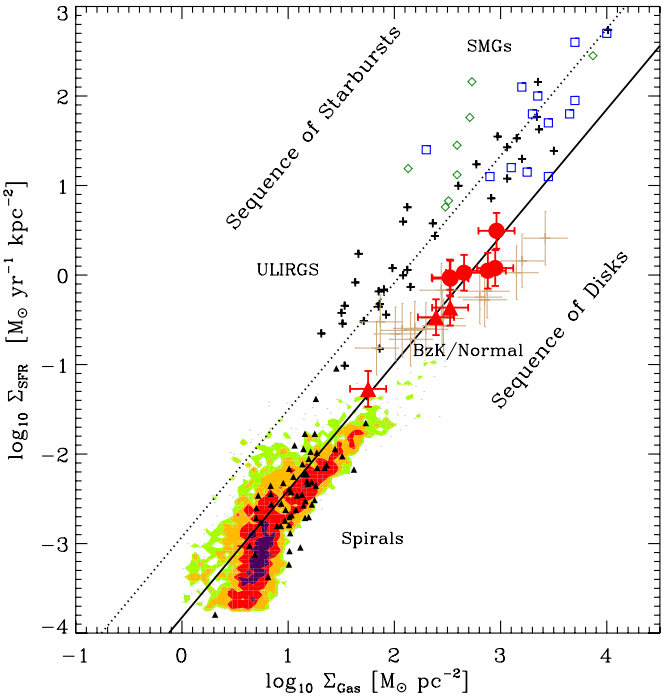

Figure 2. SFR density as a function of the gas (atomic and molecular) surface density. Red filled circles and triangles are the BzKs (D10; filled) and $z \sim 0.5$ disks (F. Salmi et al. 2010, in preparation), brown crosses are $z = 1$–2.3 normal galaxies (Tacconi et al. 2010). The empty squares are SMGs: Bouché et al. (2007; blue) and Bothwell et al. (2009; light green). Crosses and filled triangles are (U)LIRGs and spiral galaxies from the sample of K98. The shaded regions are THINGS spirals from Bigiel et al. (2008). The lower solid line is a fit to local spirals and $z = 1.5$ BzK galaxies (Equation (2), slope of 1.42), and the upper dotted line is the same relation shifted up by 0.9 dex to fit local (U)LIRGs and SMGs. SFRs are derived from IR luminosities for the case of a Chabrier (2003) IMF.

(A color version of this figure is available in the online journal.)

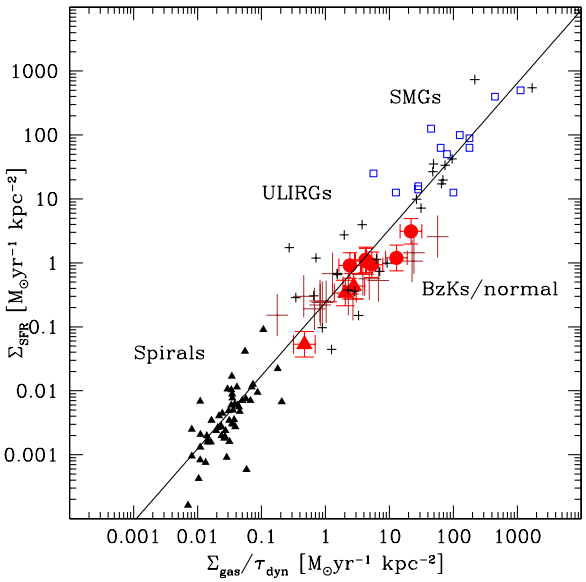

Figure 3. Same as Figure 2, but with the gas surface densities divided by the dynamical time. The best-fitting relation is given in Equation (3) and has a slope of 1.14.

(A color version of this figure is available in the online journal.)

measured at a higher signal-to-noise ratio. Again, we find that the populations are split in this diagram and are not well fit by a single sequence. Our fit to the local spirals and the BzK galaxies is virtually identical to the original K98 relation:

$$\log \Sigma_{\rm SFR}/[M_\odot\ {\rm yr}^{-1}\ {\rm kpc}^{-2}] = 1.42 \times \log \Sigma_{\rm gas}/[M_\odot\ {\rm pc}^{-2}] - 3.83. \quad (2)$$

The slope of 1.42 is slightly larger than that of Equation (1), with an uncertainty of 0.05. The scatter along the relation is 0.33 dex. Local (U)LIRG and SMGs/QSOs are consistent with a relation having a similar slope and normalization higher by 0.9 dex, and a scatter of 0.39 dex.

Despite their high SFR $\gtrsim 100\,M_\odot$ yr^{-1} and $\Sigma_{\rm SFR} \gtrsim 1\,M_\odot$ yr^{-1} kpc^{-2}, BzK galaxies are not starbursts, as their SFR can be sustained over timescales comparable to those of local spiral disks. On the other hand, M82 and the nucleus of NGC 253 are prototypical starbursts, although they only reach an SFR of a few $M_\odot$ yr^{-1}. Following Figures 1 and 2, and given the ~1 dex displacement of the disk and starburst sequences, a *starburst* may be quantitatively defined as a galaxy with $L_{\rm IR}$ (or $\Sigma_{\rm SFR}$) exceeding the value derived from Equation (1) (or Equation (2)) by more than 0.5 dex.

The situation changes substantially when introducing the dynamical timescale ($\tau_{\rm dyn}$) into the picture (Silk 1997; Elmegreen 2002; Krumholz et al. 2009; Kennicutt 1998). In Figure 3, we compare $\Sigma_{\rm gas}/\tau_{\rm dyn}$ to $\Sigma_{\rm SFR}$. Measurements for spirals and (U)LIRGs are from K98, where $\tau_{\rm dyn}$ is defined to be the rotation timescale at the galaxies' outer radius (although Krumholz et al. 2009 use the free-fall time). For the near-IR/optically selected $z = 0.5$–2.3 galaxies, we evaluate similar quantities at the half-light radius. Extrapolating the measurements to the outer radius would not affect our results substantially. Quite strikingly, the location of normal high-z galaxies is hardly distinguishable from that of local (U)LIRGs and SMGs. All observations are well described by the following relation:

$$\log \Sigma_{\rm SFR}/[M_\odot\ {\rm yr}^{-1}\ {\rm kpc}^{-2}] = 1.14 \times \log \Sigma_{\rm gas}/\tau_{\rm dyn}/[M_\odot\ {\rm yr}^{-1}\ {\rm kpc}^{-2}] - 0.62, \quad (3)$$

with a slope error of 0.03 and a scatter of 0.44 dex. The remarkable difference with respect to Figures 1 and 2 is due to the fact that the normal high-z disk galaxies have much longer dynamical timescales (given their large sizes) than local (U)LIRGs.

We can test if this holds also for integrated quantities by dividing the gas masses in Figure 1 by the average (outer radius) dynamical timescale in each population. Spirals and (U)LIRGs (whose $\tau_{\rm dyn}$ does not depend on luminosity) have average values of $\tau_{\rm dyn} = 370$ Myr and $\tau_{\rm dyn} = 45$ Myr, respectively (K98). This can be compared to $\tau_{\rm dyn} = 33$ Myr for SMGs (Tacconi et al. 2006; Bouché et al. 2007). For the QSOs, we use the SMG value. Assuming a flat rotation curve for BzKs, we get an average $\tau_{\rm dyn} = 330$ Myr at the outer radius, about three times longer than at the half-light radius, given that for an exponential profile 90% of the mass is enclosed within ~3 half-light radii. A similar value is found for our $z = 0.5$ disk galaxies and the $z = 1$–2.3 objects from Tacconi et al. (2010). Despite this simple approach, Figure 4 shows a remarkably tight trend:

$$\log {\rm SFR}/[M_\odot\ {\rm yr}^{-1}] = 1.42 \times \log(M_{\rm H2}/\tau_{\rm dyn})/[M_\odot\ {\rm yr}^{-1}] - 0.86, \quad (4)$$

with an error in slope of 0.05 and a scatter of 0.25 dex. Figure 4 suggests that roughly 10%–50% of the gas is consumed during each outer disk rotation for local spirals, and some 30%–100%

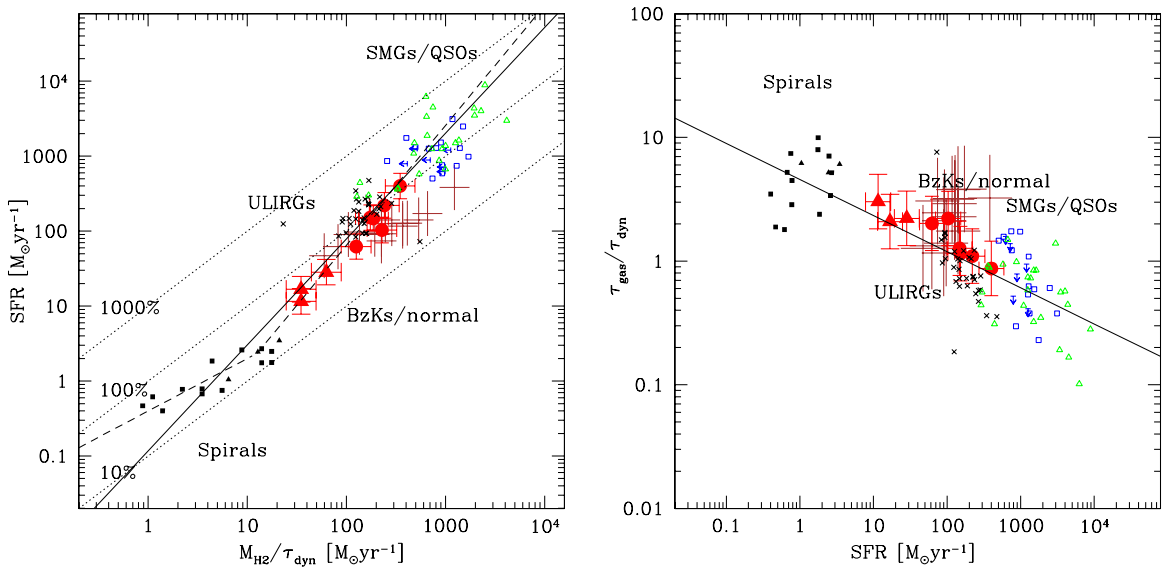

Figure 4. Same as Figure 1, but dividing the gas masses by an average estimate of the outer radius rotation timescale for the different populations. The dotted lines in the left panel show constant fractions of gas transformed into stars in each (outer radius) rotation. The best fit in the left panel (solid line; Equation (4)) has a slope of 1.42.

(A color version of this figure is available in the online journal.)

for BzK, $z = 0.5$ galaxies, and local (U)LIRGs. Some SMGs/QSOs might even consume their gas in less than one rotation.

3. DISCUSSION

The bimodal behavior in Figures 1 and 2 obviously depends on our assumptions for $\alpha_{\rm CO}$. Even though we have assumed the most accurate values that are available in the literature, one should keep in mind that this factor is still relatively poorly constrained. A possible variation of $\alpha_{\rm CO}$, e.g., as a function of galaxy properties, may change the simple picture outlined here. However, based on our current understanding, this is unlikely to greatly affect the overall conclusions. Working only with observed quantities, the BzK galaxies are already offset from local ULIRGs in the $L'_{\rm CO}/L_{\rm IR}$ diagram by a factor of 3 (D10).

In summary, the observations of near-IR selected galaxies at $z = 1.5$ do not fit a single relation of $M_{\rm gas}$ versus $L_{\rm IR}$, neither in terms of integrated quantities nor in terms of surface densities (Figures 1 and 2). There appears to be two main sequences, one for disks and one for starbursts, with the latter having 10 times higher $L_{\rm IR}$ at fixed $M_{\rm gas}$ (either integrated, or for surface densities). However, all populations define a single sequence when dividing the gas masses or surface densities by the respective dynamical timescales.

Figures 1 and 2 cannot be interpreted in terms of a single average trend for all populations with a large intrinsic scatter. Significant *systematic* shifts are observed between the BzK and $z = 0.5$–2.3 normal galaxies and other highly star-forming galaxies, such as local (U)LIRGs and SMGs. It is worth recalling here that major differences exist in the properties of local disk galaxies versus local (U)LIRGs, and the same is observed (at least on average) between distant near-IR selected BzK galaxies and SMGs (see D10, in particular Section 7.4, for a detailed discussion). Overall, this dichotomy in physical properties of spirals/(U)LIRGs and BzKs/SMGs makes it less surprising that the two classes define separate sequences in the $M_{\rm gas}/L_{\rm IR}$ plane and correspond to two distinct SF modes.

Previously it was argued that above 100 $M_\odot$ pc^{-2} the gas conversion factor would drop by a large factor (see, e.g., the discussion and references in Bouché et al. 2007; Tacconi et al. 2008). This does not seem to be the case for BzK galaxies (D10) that exhibit SF at 10 times higher gas and SFR surface densities than are seen locally. One could thus wonder how the same SF mode can be maintained at such high gas surface densities. It appears that the velocity dispersion is high in these systems (e.g., Förster Schreiber et al. 2009), probably due to high turbulence. The implication would be that BzKs have considerably thicker disks than those of local spirals. A higher gas-filling factor in BzK galaxies might also apply.

We now discuss how the observed differences in the $M_{\rm gas}$ versus $L_{\rm IR}$ plane could be interpreted. We note that the dichotomy could be altered in the $M_{\rm gas}$ versus SFR plane if stars were formed with different IMFs in disks and starbursts. For example, if the $L_{\rm IR}$ to SFR conversion factor was lower for (U)LIRGs and SMGs by a factor of 10, then if we were to plot SFR instead of $L_{\rm IR}$ in Figures 1 and 2 we would basically end up with a single SF sequence. It has been claimed that the IMF in bursts could be top heavy (e.g., Baugh et al. 2005; Elbaz et al. 1995). While the general consensus is that the appropriate IMF for local spirals is bottom light as in Chabrier (2003) or Kroupa (2002), very little is known observationally for the case of local (U)LIRGs and even less for high-redshift galaxies. In principle, the IMF might explain the bimodal behavior at least in part.

On the other hand, we have shown that the ratio of $L_{\rm IR}$ to $M_{\rm gas}$ correlates inversely with the dynamical timescales of the systems. The systematic differences disappear once the gas masses are divided by $\tau_{\rm dyn}$, given that (U)LIRGs and SMGs have much shorter $\tau_{\rm dyn}$ than disk galaxies at $0 < z < 2.3$. This is an important result because, for the first time, we show that global galaxy properties (that determine $\tau_{\rm dyn}$) are related to the regulation of a local (punctual) process like SF. The dynamical time is expected to scale with the gas volume density (ρ) as $\tau_{\rm dyn} \propto \rho^{-0.5}$ (e.g., Silk 1997). This suggests that the different $L_{\rm IR}/M_{\rm gas}$ ratios are not driven by the IMF (a difference in the

IMF would break the single relations found using τ_{dyn}) but by the fact that in some galaxies the gas can reach high volume densities and the systems can have short dynamical timescales so that the fuel is consumed more rapidly and the resulting SFR per unit of gas mass is higher. This is consistent with the existence of a unique and approximately linear correlation between L_{IR} and HCN luminosity for spirals and local (U)LIRGs (Gao & Solomon 2004; Juneau et al. 2009) and QSOs (with the exception of the highest redshift objects; Riechers et al. 2007; Gao et al. 2007). The HCN luminosity is a measure of *dense* gas, requiring H_2 volume densities $>10^4$ cm^{-3}, while CO can be thermally excited for densities $\lesssim 10^3$ cm^{-3}. Based on the HCN/L_{IR} relation, the bimodal trends of L_{IR} to M_{gas} in disks versus starbursts can be interpreted in terms of a similarly bimodal behavior for the dense gas fractions, with roughly 10 times higher fraction of dense gas in the starbursts compared to disks at fixed L_{IR} (but also with about twice higher dense gas fractions in BzKs versus local spirals). All the observations might thus be explained by a genuine increase of SFR efficiency in some galaxy classes, probably due to the concentration of the gas at high volume densities.

Major mergers or other kinds of instabilities appear to be the most natural explanation for the increased efficiencies in the starbursts (although not all mergers will necessarily produce this effect; di Matteo et al. 2008). This is not a new scenario. A higher SF efficiency in merger-driven starbursts than in rotating disks has often been implemented in semianalytical models of galaxy formation (e.g., Guiderdoni et al. 1998; Somerville et al. 2001), although this has been usually interpreted as the natural outcome of a single SF law with an exponent >1, as long as mergers make gas lose angular momentum and concentrate in the galaxy center. However, in such implementations the occurrence of very high SFRs in gas-rich disks is neglected; they thus have a bimodality in surface density, not in the SF law. Our analysis suggests that the original K98 calibration can account for the properties of disk galaxies at low and high redshifts but would underestimate the SF efficiency of starbursts by a factor of 10. An SF law with a higher exponent of 1.7 (Bouché et al. 2007) would in turn overestimate SF efficiency of gas-rich disks by a similar amount. An implementation of such a double SF law would surely influence predictions from semianalytical models of galaxy formation.

The difference in α_{CO} for disks and starbursts helps to *hide* what we are interpreting here as large differences in the SF efficiency, expressed in terms of L_{IR}/M_{gas}, by reducing the observed differences in L_{IR}/L'_{CO}. There seems to be a conspiracy at work such that the particular physical conditions that lead to high L_{IR}/M_{gas} in starbursts also determine variations in α_{CO} that obscure observationally the differences in SF efficiency. We emphasize thus that the distinction of starburst (or merging versus non merging) systems is important for interpreting CO observations, although this may be difficult on a case by case basis. We caution that blindly applying the same conversion factor to all high-z observations can lead to confusion. Also, care must be taken that SFR/IR luminosities are accurately derived. The estimates for BzK galaxies here are based on the cross-comparison of three independent SFR indicators that agree within each other very well, and overall on the global assessment by Daddi et al. (2007a, 2007b) on SFR measurements of near-IR selected galaxies at $z \sim 2$. On the other hand, purely radio selected or mid-IR selected populations are likely to produce a mixed bag of merging systems and disk galaxies and can be affected by AGNs.

We thank Adam Leroy for discussions and help with Figure 2 and Padelis Papadopoulos for discussions. We acknowledge the funding support of the ERC-StG grant UPGAL-240039, ANR-07-BLAN-0228, and ANR-08-JCJC-0008. D.R. acknowledges NASA Hubble Fellowship grant HST-HF-51235.01 awarded by the STScI, operated by AURA for NASA, contract NAS-5-26555.

REFERENCES

Baugh, C. M., Lacey, C. G., Frenk, C. S., Granato, G. L., Silva, L., Bressan, A., Benson, A. J., & Cole, S. 2005, MNRAS, 356, 1191
Bigiel, F., Leroy, A., Walter, F., Brinks, E., de Blok, W. J. G., Madore, B., & Thornley, M. D. 2008, AJ, 136, 2846
Bothwell, M. S., et al. 2009, MNRAS, 400, 154
Bouché, N., et al. 2007, ApJ, 671, 303
Chabrier, G. 2003, ApJ, 586, L133
Croton, D. J., et al. 2006, MNRAS, 365, 11
Daddi, E., Dannerbauer, H., Elbaz, D., Dickinson, M., Morrison, G., Stern, D., & Ravindranath, S. 2008, ApJ, 673, L21
Daddi, E., Dannerbauer, H., Krips, M., Walter, F., Dickinson, M., Elbaz, D., & Morrison, G. E. 2009a, ApJ, 695, L176
Daddi, E., et al. 2007a, ApJ, 670, 156
Daddi, E., et al. 2007b, ApJ, 670, 173
Daddi, E., et al. 2009b, ApJ, 694, 1517
Daddi, E., et al. 2010, ApJ, 713, 686 (D10)
Dannerbauer, H., Daddi, E., Riechers, D. A., Walter, F., Carilli, C. L., Dickinson, M., Elbaz, D., & Morrison, G. E. 2009, ApJ, 698, L178
Dekel, A., et al. 2009, Nature, 457, 451
Di Matteo, P., Bournaud, F., Martig, M., Combes, F., Melchior, A. L., & Semelin, B. 2008, A&A, 492, 31
Downes, D., & Solomon, P. M. 1998, ApJ, 507, 615
Elbaz, D., Arnaud, M., & Vangioni-Flam, E. 1995, A&A, 303, 345
Elmegreen, B. G. 2002, ApJ, 577, 206
Förster Schreiber, N. M., et al. 2009, ApJ, 706, 1364
Frayer, D. T., et al. 2008, ApJ, 680, L21
Gao, Y., Carilli, C. L., Solomon, P. M., & Vanden Bout, P. A. 2007, ApJ, 660, L93
Gao, Y., & Solomon, P. M. 2004, ApJS, 152, 63
Gnedin, N. Y., Tassis, K., & Kravtsov, A. V. 2009, ApJ, 697, 55
Greve, T. R., et al. 2005, MNRAS, 359, 1165
Guiderdoni, B., Hivon, E., Bouchet, F. R., & Maffei, B. 1998, MNRAS, 295, 877
Houghton, S., Whiteoak, J. B., Koribalski, B., Booth, R., Wiklind, T., & Wielebinski, R. 1997, A&A, 325, 923
Juneau, S., Narayanan, D. T., Moustakas, J., Shirley, Y. L., Bussmann, R. S., Kennicutt, R. C., Jr., & Vanden Bout, P. A. 2009, ApJ, 707, 1217
Kaneda, H., Yamagishi, M., Suzuki, T., & Onaka, T. 2009, ApJ, 698, L125
Kennicutt, R. C., Jr. 1998, ApJ, 498, 541 (K98)
Kroupa, P. 2002, Science, 295, 82
Krumholz, M. R., McKee, C. F., & Tumlinson, J. 2009, ApJ, 699, 850
Krumholz, M. R., & Thompson, T. A. 2007, ApJ, 669, 289
Leroy, A. K., et al. 2009, AJ, 137, 4670
McKee, C. F., & Ostriker, E. C. 2007, ARA&A, 45, 565
Monaco, P., Fontanot, F., & Taffoni, G. 2007, MNRAS, 375, 1189
Ocvirk, P., Pichon, C., & Teyssier, R. 2008, MNRAS, 390, 1326
Riechers, D. A., Walter, F., Carilli, C. L., & Bertoldi, F. 2007, ApJ, 671, L13
Riechers, D. A., et al. 2006, ApJ, 650, 604
Schmidt, M. 1959, ApJ, 129, 243
Silk, J. 1997, ApJ, 481, 703
Solomon, P. M., Downes, D., Radford, S. J. E., & Barrett, J. W. 1997, ApJ, 478, 144
Solomon, P. M., & Vanden Bout, P. A. 2005, ARA&A, 43, 677
Somerville, R. S., Primack, J. R., & Faber, S. M. 2001, MNRAS, 320, 504
Tacconi, L. J., et al. 2006, ApJ, 640, 228
Tacconi, L. J., et al. 2008, ApJ, 680, 246
Tacconi, L. J., et al. 2010, Nature, 463, 781
Weiß, A., Neininger, N., Hüttemeister, S., & Klein, U. 2001, A&A, 365, 571
Wilson, C. D., et al. 2009, ApJ, 693, 1736